

Cooperative structural and Peierls transition of indium chains on Si(111)

Y. J. Sun,^{1,2} S. Agario,¹ S. Souma,^{1,3,4} K. Sugawara,¹ Y. Tago,¹ T. Sato,¹ and T. Takahashi^{1,3}¹Department of Physics, Tohoku University, Sendai 980-8578, Japan²Department of Physics, Tsinghua University, Beijing 100084, China³WPI Research Center, Advanced Institute for Materials Research, Tohoku University, Sendai 980-8577, Japan⁴CREST, Japan Science and Technology Agency (JST), Kawaguchi 332-0012, Japan

(Received 9 November 2007; published 12 March 2008)

We have performed high-resolution angle-resolved photoemission spectroscopy on quasi-one-dimensional indium chains on the Si(111) surface to study the temperature-induced metal-insulator (MI) transition accompanied by the 4×1 to 8×2 structural change. The band dispersion near E_F shows an abrupt change at 120 K, giving a relatively large energy gap compared to the energy scale of the transition temperature. The band dispersion of the 8×2 phase shows no discernible temperature evolution, in sharp contrast to the conventional simple Peierls or structural transition. The experimental results suggest that the Peierls instability is important in the MI transition, while other structural effects are cooperatively involved.

DOI: 10.1103/PhysRevB.77.125115

PACS number(s): 71.30.+h, 71.45.Lr, 73.20.-r, 79.60.-i

One-dimensional (1D) electron systems have been a target of intensive theoretical and experimental studies since they show a variety of anomalous physical properties, such as the Tomonaga-Luttinger liquid,¹ the spin-charge separation,² and the charge- or spin-density wave (CDW or SDW) due to the Peierls instability.³ Recently, an unusual metal-insulator (MI) transition was found in quasi-1D indium (In) zigzag chains formed on the Si(111) surface.⁴ It has been recognized that the MI transition is beyond the description based on a simple CDW picture⁴⁻¹⁰ since (i) the nesting condition of 1D Fermi surfaces in the high temperature (4×1) phase is poor, (ii) the energy gap is fairly large (0.1–0.3 eV) compared to the transition temperature T_c of ~ 120 K, and (iii) the band structure near E_F is significantly different between the 4×1 and 8×2 phases. As a possible scenario for the MI transition, the temperature-induced structural transition in the indium chains with “trimer” or “hexagon” units has been proposed from the band structure calculations.¹¹⁻¹⁴ A recent angle-resolved photoemission spectroscopy⁸ (ARPES) has proposed the multiband CDW transition, where the interband charge transfer takes place to modify the Fermi surface so as to be more favorable to the commensurate nesting, although the mechanism of the interband charge transfer has not been well elucidated. Thus, the origin of the MI transition in the quasi-1D indium chains on the Si(111) surface is still highly controversial, requesting further experimental and theoretical inputs to distinguish the possible scenarios.

In this paper, we report the results of ultrahigh-resolution ARPES on the In/Si(111) surface. We measured the precise temperature dependence of the band dispersions near E_F and the Fermi surface, and we found that the band structure near E_F changes very abruptly at the MI transition temperature, giving a relatively large insulating gap in comparison to the transition temperature. We also found that the insulating gap shows no discernible temperature evolution. Based on the present ARPES results, we discuss the mechanism and origin of the anomalous MI transition in the quasi-1D indium chains on the Si(111) surface.

The single domain Si(111)(4×1)-In surface was prepared by depositing 1.2 monolayer In atoms onto a well ordered

Si(111)(7×7) at room temperature and subsequent annealing at 400 °C for 90 s. The phase transition from the 4×1 to the 8×2 superstructure at around 120 K was confirmed by low-energy electron diffraction. ARPES measurements were performed using a SCIENTA SES-2002 spectrometer with the He $I\alpha$ (21.218 eV) resonance line. The energy and angular resolution were set at 15 meV and 0.2° , respectively. The temperature of the sample was controlled by the resistive heater embedded in the sample substrate of the liquid-He cryostat and monitored by silicon-diode sensors with an accuracy of ± 0.5 K.

Figure 1 shows the experimentally determined Fermi surface of the In/Si(111)-(4×1) surface at 295 K, which was obtained by integrating the ARPES spectral intensity near E_F ($E_F \pm 30$ meV) and by plotting it as a function of two-dimensional wave vector. Bright areas correspond to the Fermi surface. There are three different quasi-1D Fermi surfaces (M_1 , M_2 , and M_3) in good agreement with previous ARPES reports,^{4,6} and all of them extend perpendicular to the chain (ΓY direction), indicative of the 1D nature of the indium chains. It is remarked that all three Fermi surfaces

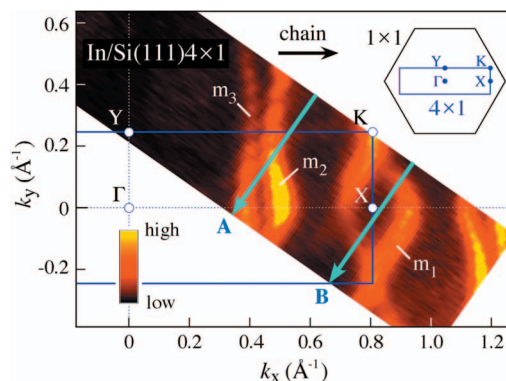


FIG. 1. (Color) ARPES intensity plot at E_F ($E_F \pm 30$ meV) as a function of two-dimensional wave vector measured with He $I\alpha$ resonance line at 295 K. The inset shows the BZ of Si(111)1 \times 1 and In(4×1). Light blue arrows show the momentum region where the ARPES spectra in Fig. 3 are measured.

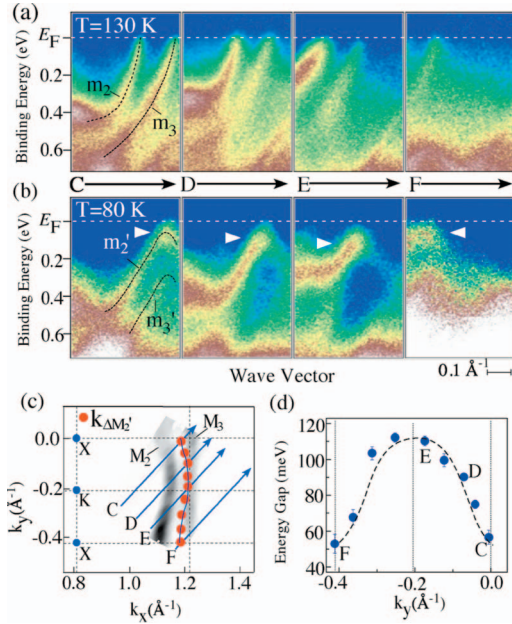


FIG. 2. (Color) Band dispersion at various cuts shown in (c) at (a) 130 K and (b) 80 K. (c) Location of cuts C–F in the BZ together with the minimum gap locus of band m_2' (red circles). The gray area corresponds to the Fermi surfaces M_2 and M_3 . (d) Momentum dependence of the gap size for band m_2' determined by plotting the energy position of the peak at the minimum gap locus.

show a small wiggling, and the wiggling is largest in the Fermi surface M_1 , while the Fermi surface M_3 exhibits a negligible wiggling, suggestive of the nearly perfect 1D nature. It is also remarked that the Fermi surface M_3 is situated at almost a half point of the Brillouin zone (BZ) and seems to satisfy the nesting condition of the commensurate $\times 2$ structure parallel to the chain.

Figures 2(a) and 2(b) show ARPES intensity plots near E_F as a function of binding energy and wave vector at tempera-

tures above and below T_c (130 and 80 K), measured along four cuts in the BZ [cuts C–F in Fig. 2(c)]. Along cuts C–E at $T=130$ K [Fig. 2(a)], we clearly find two highly dispersive bands m_2 and m_3 (Ref. 4) that apparently cross E_F . These bands m_2 and m_3 correspond to the Fermi surface of M_2 and M_3 in Fig. 1, respectively. On the other hand, at $T=80$ K, the bands do not reach E_F and disperse back toward higher binding energy, confirming the insulating nature of the 8×2 phase. According to the previous ARPES works,^{4,5,8} these two bands in cut C are attributed to bands m_2' and m_3' , respectively. While the overall band dispersion is significantly altered across the phase transition, these two bands correspond to the bands m_2 and m_3 observed above T_c .⁴ In Fig. 2(b), we denote the top of the dispersion of band m_2 by a white triangle for each cut. The minimum gap locus is shown by red circles in Fig. 2(c). As is evident from Fig. 2(b), the gap size appears to be different for each cut, indicating the substantial momentum variation of the gap. We plot in Fig. 2(d) the momentum dependence of gap size as a function of k_y . It is apparent that the gap size shows a maximum at $k_y = -0.2$ \AA^{-1} (KY cut in BZ), while it shows the minimum at $k_y = 0$ and -0.4 \AA^{-1} (ΓX cut). This marked variation of the gap size, together with the finite wiggling of the minimum gap locus of band m_2' [Fig. 2(c)], is consistent with the previous ARPES reports,⁸ suggesting that the Peierls instability plays an important role in the gap opening. Note that we observe an energy gap in all the momentum region, contrary to the previous proposal of the semimetallic ground state.¹⁵

In Figs. 3(a) and 3(b), we show the temperature dependence of the band structure near E_F measured along two cuts in the BZ (cuts A and B in Fig. 1), where the dispersion of bands m_1 – m_3 are most clearly visible. As shown in Fig. 3(a), there are two dispersive bands (m_2 and m_3) near E_F at 295 K in cut A. On decreasing temperature from 295 K, these two bands show almost no temperature dependence down to 130 K. However, at 120 K, band m_2 suddenly becomes obscure and, at the same time, band m_3 appears to be enhanced with a slight downward bending at about 0.1 eV. With a

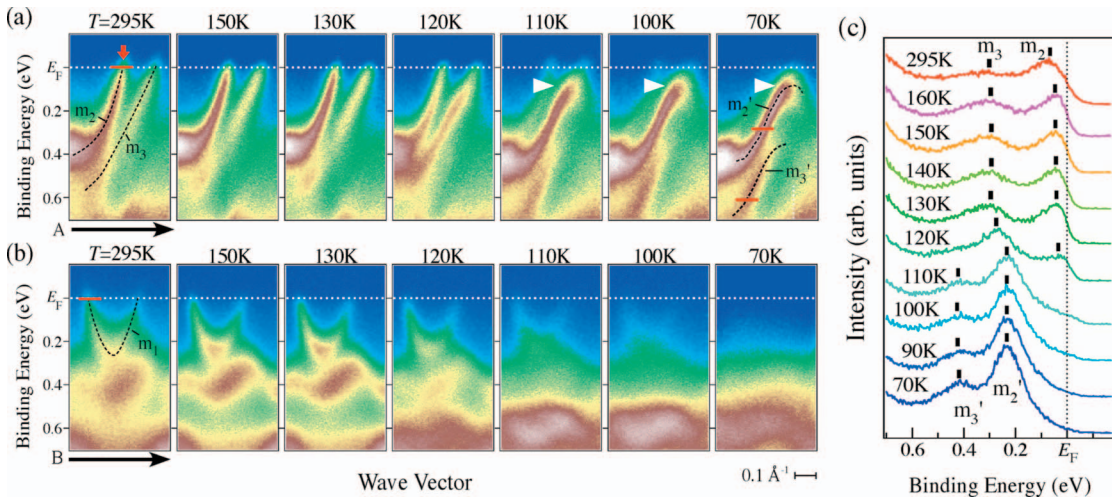


FIG. 3. (Color) (a) and (b) Temperature dependence of band dispersions near E_F measured along cuts A and B shown in Fig. 1. Dashed black lines at $T=295$ and 70 K show the position of each band determined by the peak position of the energy distribution curve (EDC). Red lines denote the regions where MDCs in Fig. 4 were measured. (c) Temperature dependence of EDC measured at the momentum location shown by a red arrow in (a). Black bars show the peak position of each spectrum.

further decrease of the temperature to 110 K by only 10 K, band m_2 becomes very faint and almost disappears, while a very strong m_2' band appears at almost the same momentum and binding energy of the band m_3 . Even when we further decrease the temperature, both bands m_2' and m_3' show no remarkable change in the location, while the intensity looks slightly enhanced at low temperatures. When we compare the band dispersions at 70 K with those at 295 K, we conclude that both bands m_2 and m_3 are simultaneously shifted downward at around 120 K and have a relatively large energy gap (80 meV for m_2' and 340 meV for m_3') near the BZ boundary below the MI transition temperature. In contrast to cut A, we find only one band (band m_1) near E_F in cut B as seen in Fig. 3(b). This band forms a small electron pocket with the bottom of about 0.2 eV and corresponds to the Fermi surface M_1 in Fig. 1. Similar to bands m_2 and m_3 in Fig. 3(a), band m_1 shows an abrupt change at around 120 K. The intensity of band m_1 suddenly becomes weak at 120 K and the band itself totally disappears at 70 K. By considering the charge conservation across the MI transition, the m_1' band would be located above E_F at temperatures below T_c , since bands m_2' and m_3' are fully occupied and accommodate more electrons than the partially occupied bands m_2 and m_3 .^{8,13,14} All these experimental results on the band structure near E_F are essentially consistent with the previous ARPES reports^{5,8,16} and further reveal that a sudden phase transition takes place at around 120 K.

To clarify the temperature dependence of the band dispersion more quantitatively, we show in Fig. 3(c) the ARPES spectra measured at the Fermi vector (k_F) of band m_2 shown by a red arrow in Fig. 3(a). We observe two prominent peaks at each temperature as indicated by black bars. Two peaks at E_F and 300 meV in the spectra above 120 K are attributed to bands m_2 and m_3 , while those at 220 and 420 meV below 110 K correspond to bands m_2' and m_3' . As clearly seen in Fig. 3(c), the peak position of bands above 120 K or below 110 K is temperature independent and seems to suddenly shift at 110–120 K. We do not find any additional features between E_F and 220 meV or between 300 and 420 meV, indicative of the presence of intermediate bands that smoothly connect bands m_2 (m_3) and m_2' (m_3'). The observed abrupt change of the band dispersion at T_c suggests the first-order nature of the MI transition of indium chains, consistent with the previous scanning tunneling microscopy (STM) experiment.¹⁷ The size of the energy gap in the 8×2 phase shows a negligible temperature dependence as seen in Fig. 3(c). These experimental results seem to be hardly explained in terms of a simple CDW or a simple structural transition. It is also noted that no sign of spectral broadening is observed above T_c as in a previous ARPES study,¹⁶ which rules out the possibility of dynamical fluctuation at high temperature.¹⁸ The above anomalous spectral behaviors together with the temperature-induced overall change of the band structure across T_c appear to be consistent with the recent theoretical studies,^{13,14} which suggest that the displacement of two zig-zag indium chains caused by the shear distortion significantly alters the band structure to trigger the Peierls instability. Considering the large gap size of band m_2 , it is inferred that the CDW transition temperature of the shear-distorted state would be remarkably high (< 500 K), but the shear-

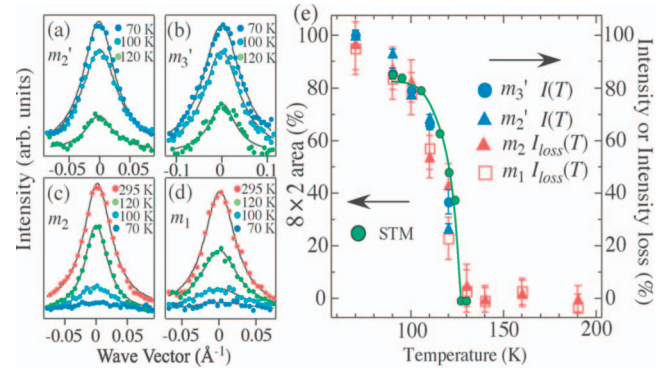


FIG. 4. (Color) (a)–(d) Temperature dependence of MDCs measured at locations shown by red lines in Figs. 3(a) and 3(b). (e) Temperature dependence of normalized ARPES intensity for bands m_2' and m_3' , and the normalized intensity loss for bands m_2 and m_3 . Green circles show the ratio of 8×2 area at various temperatures determined by STM (Ref. 17).

distorted state involving the Peierls instability would be energetically unstable above 120 K with respect to the metallic 4×1 state. On decreasing the temperature, the shear-distorted state may become more stable than the 4×1 state at around 120 K and undergo an abrupt transition at 120 K accompanied with a large Peierls-gap opening. It is remarked here that the conventional Peierls transition also involves the structural transition because electron and lattice degrees of freedom are coupled to each other. The main difference in the present system as compared to such conventional systems is that the structural transition itself significantly modifies the original band structure, causing the different nesting condition of the Fermi surface across T_c and the abrupt opening of an energy gap at T_c , while in the conventional system, the nesting condition of a normal-state Fermi surface is well retained even below T_c and the gap gradually evolves with decreasing temperature.

It is noted that the intensity of the metallic bands m_1 , m_2 , and m_3 does not completely vanish even below T_c (120–100 K) as shown in Fig. 3. Based on the experimental fact that the 4×1 and 8×2 phases coexist even below T_c due to the local defects as revealed by STM,^{15,17} it is inferred that the residual intensity of bands m_1 – m_3 in the ARPES experiment may reflect the finite signal from the remaining 4×1 domains below T_c . To compare quantitatively the ARPES and STM results, we have estimated the temperature dependence of the ARPES spectral weight $I(T)$ for bands m_2' , m_3' , m_2 , and m_1 by fitting the momentum distribution curves (MDCs) with a Lorentzian. We plot in Fig. 4(e) the normalized intensity $I(T)/I(70)$ for bands m_2' and m_3' , and the normalized intensity loss defined as $[I(295) - I(T)]/I(295)$ for bands m_1 and m_2 . As clearly seen in Fig. 4(e), the intensity and the intensity loss show an almost the same temperature dependence. They are nearly zero down to 130 K and start to increase at 120 K. This temperature dependence of the ARPES intensity shows good agreement with that of the spatial occupation ratio of the 8×2 phase observed by the STM measurement (green circles),¹⁷ suggesting that the simultaneous observation of metallic and insulating bands at 100–120 K in ARPES measurement [Fig. 3(a)] is attributed

to the coexistence of the 4×1 and 8×2 phases.

In conclusion, the present high-resolution ARPES results have revealed the precise temperature dependence of the band dispersions near E_F in the quasi-1D indium chains on the Si(111) surface. The band dispersions show an abrupt change at around T_c (120 K), producing a relatively large energy gap at E_F compared to the energy scale of T_c at low temperatures. We found that the size of the gap shows a

negligible temperature dependence. We have proposed that the anomalous MI transition of indium chains on Si(111) is caused by the cooperative effect of the Peierls and other structural transitions.

We thank K. Sakamoto for his suggestions on the sample preparation. This work was supported by grants from JSPS, JST-CREST, and MEXT of Japan.

-
- ¹J. M. Luttinger, *J. Math. Phys.* **4**, 1154 (1963).
²E. H. Lieb and F. Y. Wu, *Phys. Rev. Lett.* **20**, 1445 (1968).
³R. E. Peierls, *Quantum Theory of Solids* (Clarendon, Oxford, 1964).
⁴H. W. Yeom, S. Takeda, E. Rotenberg, I. Matsuda, K. Horikoshi, J. Schaefer, C. M. Lee, S. D. Kevan, T. Ohta, T. Nagao, and S. Hasegawa, *Phys. Rev. Lett.* **82**, 4898 (1999).
⁵O. Gallus, Th. Pillo, M. Hengsberger, P. Segovia, and Y. Baer, *Eur. Phys. J. B* **20**, 313 (2001).
⁶T. Abukawa, M. Sasaki, F. Hisamatsu, T. Goto, T. Kinoshita, A. Kakizaki, and S. Kono, *Surf. Sci.* **325**, 33 (1995).
⁷T. Tanikawa, I. Matsuda, T. Kanagawa, and S. Hasegawa, *Phys. Rev. Lett.* **93**, 016801 (2004).
⁸J. R. Ahn, J. H. Byun, H. Koh, E. Rotenberg, S. D. Kevan, and H. W. Yeom, *Phys. Rev. Lett.* **93**, 106401 (2004).
⁹S. J. Park, H. W. Yeom, S. H. Min, D. H. Park, and I.-W. Lyo, *Phys. Rev. Lett.* **93**, 106402 (2004).
¹⁰C. Kumpf, O. Bunk, J. H. Zeysing, Y. Su, M. Nielsen, R. L. Johnson, R. Feidenhans'l, and K. Bechgaard, *Phys. Rev. Lett.* **85**, 4916 (2000).
¹¹J.-H. Cho, J.-Y. Lee, and L. Kleinman, *Phys. Rev. B* **71**, 081310(R) (2005).
¹²A. A. Stekolnikov, K. Seino, F. Bechstedt, S. Wippermann, W. G. Schmidt, A. Calzolari, and M. B. Nardelli, *Phys. Rev. Lett.* **98**, 026105 (2007).
¹³C. Gonzalez, J. Ortega, and F. Flores, *New J. Phys.* **7**, 100 (2005).
¹⁴S. Riikonen, A. Ayula, and D. Stachez-Portal, *Surf. Sci.* **600**, 3821 (2006).
¹⁵J. Guo, G. Lee, and E. W. Plummer, *Phys. Rev. Lett.* **95**, 046102 (2005).
¹⁶J. R. Ahn, J. H. Byun, J. K. Kim, and H. W. Yeom, *Phys. Rev. B* **75**, 033313 (2007).
¹⁷S. J. Park, H. W. Yeom, J. R. Ahn, and I.-W. Lyo, *Phys. Rev. Lett.* **95**, 126102 (2005).
¹⁸C. Gonzalez, F. Flores, and J. Ortega, *Phys. Rev. Lett.* **96**, 136101 (2006).